



Article

Truck Handling Stability Simulation and Comparison of Taper-Leaf and Multi-Leaf Spring Suspensions with the Same Vertical Stiffness

Leilei Zhao 1 , Yunshan Zhang 2 , Yuewei Yu 1,* , Changcheng Zhou 1,* , Xiaohan Li 1 and Hongyan Li 3

- School of Transportation and Vehicle Engineering, Shandong University of Technology, Zibo 255000, China; zhaoleilei611571@163.com (L.Z.); xhan_lee@163.com (X.L.)
- Shandong Automobile Spring Factory Zibo Co., Ltd., Zibo 255000, China; dyn_keylab@163.com
- State Key Laboratory of Automotive Simulation and Control, Jilin University, Changchun 130022, China; shanligongdaxue@126.com
- * Correspondence: yuyuewei2010@163.com (Y.Y.); greatwall@sdut.edu.cn (C.Z.); Tel.: +86-135-7338-7800 (C.Z.)

Received: 16 December 2019; Accepted: 31 January 2020; Published: 14 February 2020



Abstract: The lightweight design of trucks is of great importance to enhance the load capacity and reduce the production cost. As a result, the taper-leaf spring will gradually replace the multi-leaf spring to become the main elastic element of the suspension for trucks. To reveal the changes of the handling stability after the replacement, the simulations and comparison of the taper-leaf and the multi-leaf spring suspensions with the same vertical stiffness for trucks were conducted. Firstly, to ensure the same comfort of the truck before and after the replacement, an analytical method of replacing the multi-leaf spring with the taper-leaf spring was proposed. Secondly, the effectiveness of the method was verified by the stiffness tests based on a case study. Thirdly, the dynamic models of the taper-leaf spring and the multi-leaf spring with the same vertical stiffness are established and validated, respectively. Based on this, the dynamic models of the truck before and after the replacement were established and verified by the steady static circular test, respectively. Lastly, the handling stability indexes for the truck were compared by the simulations of the drift test, the ramp steer test, and the step steer test. The results show that the yaw rate of the truck almost does not change, the steering wheel moment decreases, the vehicle roll angle obviously increases, and the vehicle side slip angle slightly increases after the replacement. Thus, the truck with the taper-leaf spring suspension has better steering portability, however, its handling stability performs worse.

Keywords: trucks; handling stability; lightweight; taper-leaf spring; suspension; step steer

1. Introduction

The handling stability is one of the extremely important performances that affect the driving safety of trucks. How to obtain the strong handling stability for improving the driving safety is an important issue in vehicle design [1–3]. The suspension is an important system connecting the truck frame and wheel [4]. The leaf spring is the most widely used elastic element in the suspension system for trucks. Moreover, it plays a crucial role in the handling stability for trucks.

At present, the lightweight design of trucks is of great importance to enhance the load capacity and reduce the production cost [5–7]. For leaf springs, the lightweight design of trucks is mainly reflected in replacing the multi-leaf spring with the taper-leaf spring, so as to reduce the trucks' weight, to improve the power performance, and to reduce the fuel consumption and the exhaust pollution [8–10]. In modern society, with the development of people's living standard, people have higher and higher

Appl. Sci. 2020, 10, 1293 2 of 21

requirements for the handling stability of trucks [11–13]. However, the changes of the handling stability after the replacement have not been revealed.

Due to the advantages of light weight and low noise, the taper-leaf spring is more and more used in trucks. At present, scholars mainly focus on its dynamic property, stress, and strain. Moreover, most of the studies of its mechanical properties mainly were conducted by using simulation software packages, such as Ansys, Nastran, Abaqus, and Adams. Duan et al. created the dynamic model of the tandem suspension equipped with the taper leaf spring for trucks based on Adams software [14]. In order to research the stress of a taper leaf spring, Moon et al. established a flexible multi-body dynamic model [15]. Wang et al. proposed a calculation method of the stiffness of the taper-leaf spring based on the combine superposition method and the finite difference method [16]. Zhou et al. analyzed the mechanical properties of the taper leaf spring considering the friction between the leaf springs on the basis of the FE (Finite Element) contact analysis [17]. To improve the kinematics characteristics of a midsize truck, Kim et al. selected the optimal combination parameters based on a vehicle model with a taper leaf spring [18].

Some scholars improved the performance of leaf springs from the perspective of materials. For example, Chandra et al. researched the high-temperature quality of the accelerated spheroidization on SUP9 leaf spring and the machining performance of Sup9 leaf spring can be significantly improved under high temperature [19]. Fragoudakis et al. optimized the development of 56SiCr7 leaf springs and micro-hardness measurements show surface degradation effects [20]. Kumar et al. optimized the key design parameters of EN45A flat leaf spring and the developed leaf spring program can be used to optimize various parameters of the leaf spring quickly and reliably [21]. Jenarthanan proposed carbon/glass epoxy composite as a leaf spring material and analyzed the leaf spring by using Ansys software [22]. Ozmen et al. proposed a new method on the basis of testing and simulation for the durability of leaf springs [23]. In their study, the finite element method and the multi-body simulation were used to calculate the fatigue life. Some scholars researched the fatigue life of leaf springs. For example, Duruş et al. proposed a method to predict the fatigue life of Z Type leaf spring and created an approach to validate the proposed method [24]. Bakir et al. researched the correlation of simulation, test bench, and rough road testing in terms of strength and fatigue life of a leaf spring [25]. Kong et al. conducted the failure evaluation of a leaf spring eye design under various load cases [26] and this study provides a valuable reference for preventing the failure of leaf spring in engineering design. Bi et al. carried out the fatigue analysis of leaf-spring pivots [27]. Malikoutsakis proposed the design and optimization procedure for parabolic leaf springs and made a multi-disciplinary optimization of the high performance front leaf springs [28]. In addition, some scholars researched the influences of the taper-leaf spring on the vehicle performances. For instance, Liu et al. analyzed the effects of the taper-leaf spring on the vehicle braking property, simulated the motion characteristics of the front less leaf spring suspension system and the motion law of the front axle jumping up with the wheel [29]. Liu et al. researched the main leaf center trajectory of the taper leaf spring and analyzed the suspension kinematics, and unreasonable toe-in angle was solved by optimizing the hard point of the plumbing arm [30].

In addition, some scholars focus on the influence of suspension designs on handling performance. Termous et al. a proposed coordinated control strategy to control the roll dynamics on the basis of active suspension systems [31]. Li et al. applied the hydraulically interconnected suspension to an articulated vehicle and proved that it can effectively improve the vehicle handling performance [32]. In order to improve the handling stability, Zhang et al. carried out the multi-objective optimization design of suspensions for electric vehicles [33]. Bagheri et al. carried out a multi-objective optimization on the double wishbone suspension to improve the vehicle handling stability [34]. A linear mathematical model and MATLAB model which included suspension K and C characteristics parameters were established by Li et al. [35]. Moreover, the accuracy of the mathematical model was validated. Ahmadian et al. discussed an application of magneto-rheological (MR) suspensions about vehicle

Appl. Sci. 2020, 10, 1293 3 of 21

handling stability and their results show that using MR suspensions can increase the speed at which the onset of hunting occurs as much as 50% to more than 300% [36].

The above-mentioned studies provide theoretical guidance for the application and promotion of the taper-leaf spring in vehicles. They also provide a useful reference for the theoretical research of the taper-leaf spring. They mainly focus on the mechanical properties of the taper-leaf itself. There is no research focusing on the changes of the handling stability after replacing the multi-leaf spring with the taper-leaf spring for trucks. The study of the changes will help to optimize the design of the suspension system and improve the handling stability for trucks. Thus, the changes need to be further researched.

The aim of this paper is to reveal the changes of the handling stability after replacing the multi-leaf spring with the taper-leaf spring for trucks. The main contributions of this paper are as follows: (1) An analytical method of replacing the multi-leaf spring with the taper-leaf spring was proposed and validated by test. (2) The dynamic models of the truck before and after the spring replacement were established and verified by tests, respectively. (3) The changes of the handling stability after replacing the multi-leaf spring with the taper-leaf spring were revealed by the simulations of the drift test, the ramp steer test, and the step steer test.

2. Modeling of the Taper-Leaf and the Multi-Leaf Spring

2.1. The Mechanical Model of the Multi-Leaf Spring

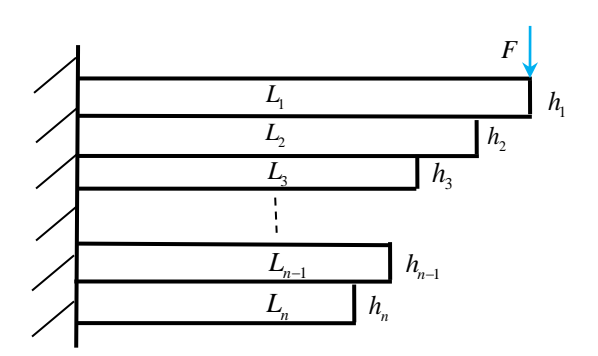


Figure 1. The mechanical model of the multi-leaf spring.

Based on the mechanical model in Figure 1, the stiffness of the half of the multi-leaf spring can be expressed as [37]:

$$K = \frac{bE}{4} / \left[\sum_{i=2}^{n} \frac{(L_1 - L_i)^3 - (L_1 - L_{i-1})^3}{h_1^3 + h_2^3 + \dots + h_{i-1}^3} + \frac{L_1^3 - (L_1 - L_n)^3}{h_1^3 + h_2^3 + \dots + h_{n-1}^3 + h_n^3} \right], \tag{1}$$

where *E* is the elastic modulus.

2.2. The Mechanical Model of the Single Taper-Leaf Spring

The half of the single taper-leaf spring is taken as the research object. Its mechanical model is shown in Figure 2. Similarly, the half of the single taper-leaf spring also can be regarded as an

Appl. Sci. 2020, 10, 1293 4 of 21

elastic beam. It is fixed at one end. A concentrated load F is applied at the other end. The geometric parameters and the coordinate system are marked in Figure 2. L is the half length of the single taper-leaf spring; h_2 is the thickness for $x \in [l_2, L]$; h_1 is the thickness for $x \in [0, l_1]$. h(x) is the thickness for $x \in [l_1, l_2]$. γ is defined as the thickness ratio and $\gamma = h_1/h_2$.

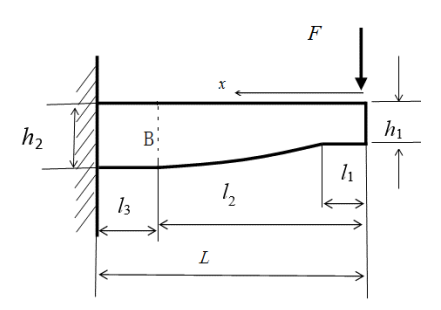


Figure 2. The mechanical model of the single taper-leaf spring.

Based on the model in Figure 2, when the load F is applied at the free end, the same normal stress at any position for $x \in [l_1, l_2]$ is [9]:

$$\sigma_x = \frac{6Fx}{bh^2(x)} \tag{2}$$

From Equation (2), the normal stress σ_B of Section B for $x = l_2$ can be expressed as:

$$\sigma_{\rm B} = \frac{6Fl_2}{bh_2^2} \tag{3}$$

In order to meet the requirements of the equal stress at Section B for $x = l_2$, $\sigma_x = \sigma_B$ must be satisfied. According to Equations (2) and (3), h(x) can be expressed as:

$$h(x) = h_2 \sqrt{\frac{x}{l_2}} \tag{4}$$

According to Equation (4), h_1 can be expressed as:

$$h_1 = h_2 \sqrt{\frac{l_1}{l_2}} \tag{5}$$

When the load *F* is applied at the free end, the deformation energy *U* can be expressed as:

$$U = \int_{L} \frac{(Fx)^{2}}{2EI} dx = \int_{0}^{l_{1}} \frac{(Fx)^{2}}{2EI_{1}} dx + \int_{l_{1}}^{l_{2}} \frac{(Fx)^{2}}{2EI_{2}} dx + \int_{l_{2}}^{L} \frac{(Fx)^{2}}{2EI_{3}} dx$$
 (6)

where I_1 , I_2 , I_3 are the inertia moments at different thicknesses and $I_1 = \frac{bh_1^3}{12}$, $I_2 = \frac{bh^3(x)}{12}$, $I_3 = \frac{bh_2^3}{12}$, respectively.

According to the Castigliano Second Theorem [37], the end deformation of the spring can be expressed as:

$$y = \frac{\partial U}{\partial F} = \frac{4F\left[L^3 + l_2^3\left(1 - \gamma^3\right)\right]}{Ebh_2^3} \tag{7}$$

Based on Equation (7), the stiffness of the half of the single taper-leaf spring can be expressed as:

$$K_{\rm s} = \frac{Ebh_2^3}{4\left[L^3 + l_2^3(1 - \gamma^3)\right]} \tag{8}$$

Appl. Sci. 2020, 10, 1293 5 of 21

According to Equation (8), the design formula of the root thickness can be expressed as:

$$h_2 = \sqrt[3]{\frac{4K_s[L^3 + l_2^3(1 - \gamma^3)]}{Eb}}$$
 (9)

2.3. The Mechanical Model of the Taper-Leaf Spring Including n Pieces

The half of the taper-leaf spring including n pieces (n = 2 or 3) is taken as the research object. Its mechanical model is shown in Figure 3. Similarly, the half of the single taper-leaf spring also can be regarded as an elastic beam. It is fixed at one end. A concentrated load F is applied at the other end. The geometric parameters and the coordinate system are marked in Figure 3. The end displacement of the taper-leaf spring is y. γ_i is defined as the thickness ratio and $\gamma_i = h_{i1}/h_{i2}$. Moreover, all the design values of γ_i are the same in practical engineering application and $\gamma_i = \gamma$.

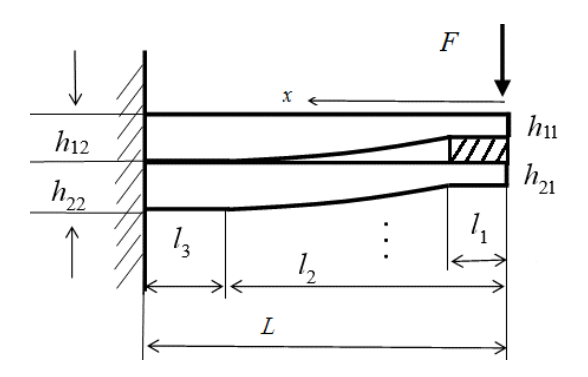


Figure 3. The mechanical model of the taper-leaf spring including n pieces.

Under the load F, each piece does not separate from each other at the free end. The free ends of the n pieces for the taper-leaf spring are equivalent to a whole body and the vertical displacement occurs under the load F. Thus, each piece has the same vertical displacement y at the free end, that is:

$$y_i = y \tag{10}$$

where y_i the displacement of the *i*th piece at the free end (i = 1, 2 or i = 1, 2, 3).

According to Equation (7), y_i can be expressed as:

$$y_i = \frac{4F_i \left[L^3 + l_2^3 \left(1 - \gamma^3 \right) \right]}{Ebh_{i2}^3} \tag{11}$$

where F_i is the load shared by the *i*th piece.

Substituting Equation (11) into Equation (10), obtain the following:

$$\frac{F_1}{h_{12}^3} = \frac{F_2}{h_{22}^3} = \dots = \frac{F_i}{h_{i2}^3} = \dots = \frac{F_n}{h_{n2}^3} = \frac{F}{h_{e2}^3}$$
 (12)

where h_{e2} is the equivalent thickness.

According to the model in Figure 3, the sum of the concentrated forces is equal to the concentrated load *F*, that is:

$$F_1 + F_2 + \dots + F_n = F \tag{13}$$

According to Equations (12) and (13), h_{e2} can be calculated by:

$$h_{e2} = \sqrt[3]{h_{12}^3 + h_{22}^3 + \dots + h_{n2}^3} \tag{14}$$

Appl. Sci. 2020, 10, 1293 6 of 21

According to Equation (12), F_i can be calculated by:

$$F_i = \frac{h_{i2}^3}{h_{e2}^3} F \tag{15}$$

Under the load *F*, the maximum normal stress of the *i*th piece can be expressed as:

$$\sigma_{i\text{max}} = \frac{6F_i L}{bh_{i2}^2} \tag{16}$$

Substituting Equation (15) into Equation (16), obtain the following:

$$\sigma_{i\max} = \frac{6FLh_{i2}}{bh_{s2}^3} \tag{17}$$

3. Analytical Method of Replacing the Multi-Leaf Spring with the Taper-Leaf Spring

This paper mainly research the changes of the handling stability after replacing the multi-leaf spring with the taper-leaf spring for trucks by comparison. Therefore, it is necessary to ensure that the two leaf springs have the same vertical stiffness. Only on this premise can the conclusions of the comparison be valuable. In addition, the design of the taper-leaf spring must meet the stress condition. In this section, an analytical method of replacing the multi-leaf spring with the taper-leaf spring under the precondition of the same vertical stiffness was proposed.

3.1. The Analytical Design Method of the Taper-Leaf Spring

For the taper-leaf spring, σ_{imax} must be not larger than the allowable stress [σ]. Thus, based on $\sigma_{imax} \leq [\sigma]$ and Equation (17), the root allowable thickness of the ith piece can be expressed as:

$$[h_{i2}] = \frac{bh_{e2}^3[\sigma]}{6FI} \tag{18}$$

According to Equation (14), when $h_{12} = h_{22} = \cdots = h_{n2}$, obtain the following:

$$h_{\rm e2}^3 = nh_{i2}^3 \tag{19}$$

According to Equation (19), the number n of the spring pieces can be expressed as:

$$n = \frac{h_{\rm e2}^3}{\left[h_{i2}^3\right]} \tag{20}$$

Based on Equation (20), rounding up n, obtain the number [n] of the spring pieces meeting stress requirements.

Substituting [*n*] into Equation (20), the design value of the root thickness of the *i*th piece can be calculated by:

$$h_{i2} = \frac{h_{e2}}{\sqrt[3]{[n]}} \tag{21}$$

According to Equation (5) and the definition of the thickness ratio γ , the design value of l_1 can be calculated by:

$$l_1 = l_2 \gamma^2 \tag{22}$$

According to the definition of the thickness ratio γ and h_{i2} , h_{i1} can be designed as:

$$h_{i1} = \gamma h_{i2} \tag{23}$$

Appl. Sci. 2020, 10, 1293 7 of 21

3.2. The Design Flow

The design flow of the analytical method of replacing the multi-leaf spring with the taper-leaf spring under the precondition of the same vertical stiffness can be summarized as follows:

- **Step 1.** By using Equation (1), calculate the stiffness *K* of the multi-leaf spring of the original vehicle.
- **Step 2.** Let $K_s = K$ and by using Equation (9), calculate the equivalent thickness h_{e2} .
- **Step 3.** Substituting h_{e2} into Equation (18), obtain the root allowable thickness [h_{i2}].
- **Step 4.** Substituting h_{e2} and $[h_{i2}]$ into Equation (20), rounding up n, obtain the number [n] of the spring pieces meeting stress requirements.
 - **Step 5.** Based on [n], by using Equation (21), obtain the root thickness h_{i2} of the *i*th piece.
 - **Step 6.** Based on γ and l_2 , by using Equation (22), obtain the length l_1 of the end segment.
 - **Step 7.** Based on γ and h_{i2} , by using Equation (23), obtain the end thickness h_{i1} of the *i*th piece.

3.3. Case Study

A light truck was selected as the research object. Its rear suspension is equipped with the multi-leaf spring. Moreover, the number of slices for the multi-leaf spring is five. The specific parameters are as follows: b=63.0 mm, h=8.0 mm, $L_1=525.0$ mm, $L_2=450.0$ mm, $L_3=350.0$ mm, $L_4=250.0$ mm, $L_5=150.0$ mm, $L_6=150.0$ mm, $L_6=150.0$ mm, $L_6=150.0$ mm, $L_6=150.0$ mm, $L_6=150.0$ mm, $L_6=150.0$ mm for the taper-leaf spring. According to $L_6=150.0$ mm for the taper-leaf spring with the taper-leaf spring, the other design parameters values were determined. The key design parameters values of the taper-leaf spring are shown in Table 1. The prototype of the taper-leaf spring manufactured by Shandong Automobile Spring Factory is shown in Figure 4.

Table 1. The design parameters values.

Parameter	Value	Unit	Parameter	Value	Unit
n	3	pieces	h_{11}	5.6	mm
$\sigma_{ ext{max}}$	460.2	MPa	h_{21}	5.6	mm
b	63.0	mm	h_{31}	5.6	mm
l_1	123.5	mm	h_{12}	11.0	mm
l_2	475.0	mm	h_{22}	11.0	mm
l_3	50.0	mm	h_{32}	11.0	mm



Figure 4. The prototype of the taper-leaf spring.

4. Dynamic Modeling and Test Verification

4.1. Dynamic Modeling and Verification of Leaf Springs

Adams is recognized as a professional software for the vehicle dynamics modeling. The dynamic models based on the software can truly reflect the dynamic performance of vehicles [38,39]. Adams/Leaf tool uses discrete beam elements to simulate leaf springs. In other words, each piece of leaf springs is divided into several sections, which are connected by flexible beams without mass. The flexible beam is a kind of flexible connection. The force and moment between two marked points of two elements are calculated by the theory of Timoshenko beam [40]. In this study, according to the structural parameters values of the multi-leaf spring and the taper-leaf spring, the simulation models were established based on Adams/Leaftool software, as shown in Figure 5. Because the friction force between the adjacent pieces is very small [37], it is ignored in the simulation models. Moreover, the previous tests in [37]

Appl. Sci. 2020, 10, 1293 8 of 21

show that the load-stiffness characteristics for multi-leaf springs and taper-leaf springs are almost linear. Thus, their vertical stiffness and the torsional stiffness are often used to verify the model accuracy [9].

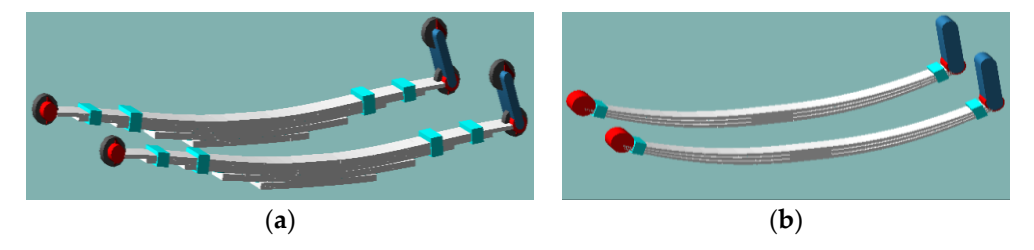


Figure 5. The simulation models: (a) The multi-leaf spring; (b) the taper-leaf spring.

To verify the accuracy of the models, the vertical and torsional stiffness tests were conducted. The test equipment is the TYE-W400I hydraulic testing machine produced by Jinan Shidai Shijin Group, as shown in Figure 6. It uses the programmable logic controller. It can measure the load and the displacement through sensors. The load was measured by a NS-WL1 tension–compression sensor. The displacement was measured by a SDVG20 displacement sensor. The control system automatically collected and processed the test force and the deformation of leaf springs, and directly output the stiffness value through the microcomputer display screen. For the models in Figure 5, the vertical forces were applied to simulate the deformation, respectively. The simulated stiffness values from the simulation results were calculated. A comparison of the stiffness values is shown in Table 2.



Figure 6. The test equipment.

Table 2. A comparison of the stiffness values.

	Vertical			Torsional		
Type	Test (kN/m)	Simulation (N/m)	Error (%)	Test (kNm/rad)	Simulation (kNm/rad)	Error (%)
The multi-leaf spring The taper-leaf spring	112.3 113.1	109.0 109.2	2.9 3.5	10.6 8.4	10.1 8.2	4.7 2.4

From Table 2, it can be seen that the vertical stiffness values of the multi-leaf spring and the taper-leaf spring are almost the same. The result shows that the taper-leaf spring can equivalently replace the original multi-leaf spring. From Table 2, it also can be seen that the torsional stiffness of the multi-leaf spring is obviously larger than that of taper-leaf spring. Moreover, the test values are close to the simulation values. The results show that the simulation models can effectively reflect the stiffness characteristics of the multi-leaf spring and the taper-leaf spring, respectively. In addition, the experimental results indicate that the weight of the taper-leaf spring is less 13.4% than that of the multi-leaf spring.

Appl. Sci. 2020, 10, 1293 9 of 21

4.2. Dynamic Modeling of the Truck

The parameters values of the light truck are shown in Table 3. The geometric model of the light truck is shown in Figure 7a. The modeling process is as follows: firstly, the geometric model is imported into Adams through the "parasolid" data format; then, system constraints, loads, and drives are applied in Adams; finally, the simulation models of the multi-leaf spring and the taper-leaf spring are imported and assembled to establish the vehicle dynamic models, respectively. The dynamic model of the truck with the multi-leaf spring is shown in Figure 7b. The tire adopts the PAC2002 tire model. This tire model adopts the magic formula, which is suitable for the simulation analysis of stability with high accuracy [41,42]. The steering system is equipped with rack-and-pinion steering gear and the angular ratio of steering gear is 18.0.

Parameter	Value	Parameter	Value
The unsprung mass for the front wheel /(kg)	46.4	The differential ratio	4.778
The front axle load /(kg)			8.3
The rear axle load /(kg)	1641	The arm length of the stabilizer /(mm)	204
The wheelbase/(m)	2.6	The bar length of the stabilizer /(mm)	910
The front tread /(m)	1.32	The front wheel radius /(m)	0.297
The rear tread /(m)	1.41	The rear wheel radius /(m)	0.297
The stiffness of the front suspension /(N/mm)	55	The front wheel stiffness /(kNm ⁻¹)	383.4
The unsprung mass for the rear wheel /(kg)	83	The rear wheel stiffness /(kNm ⁻¹)	383.4
The angular ratio of steering gear	18.0	, ,	

Table 3. The parameters values of the light truck.

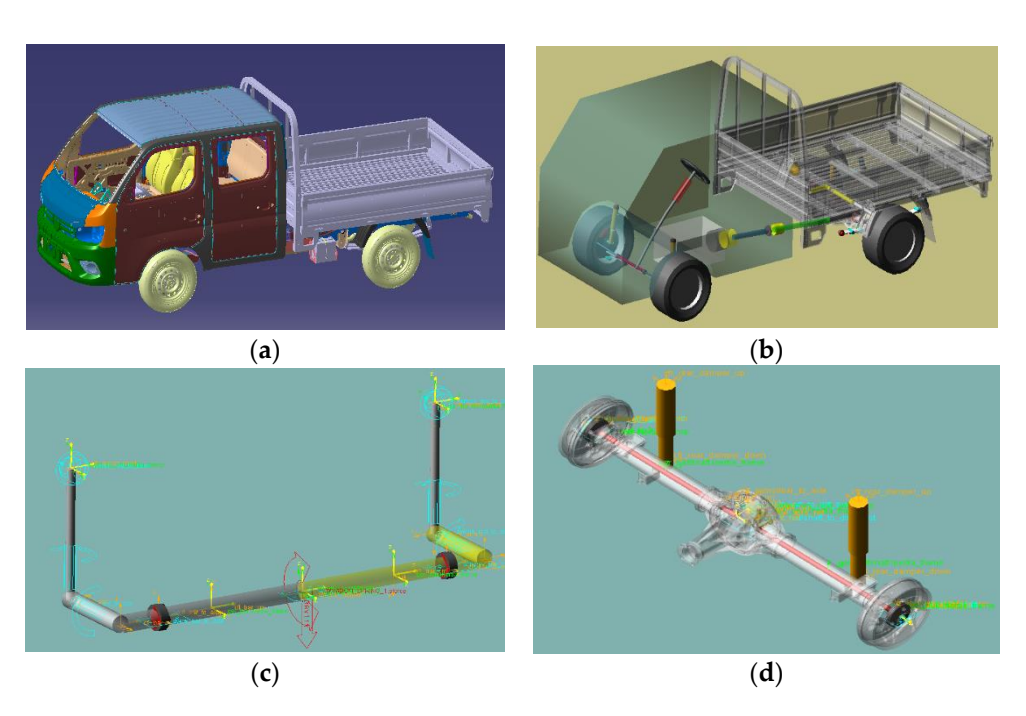


Figure 7. The light truck models: (a) The geometric model, (b) the dynamic model, (c) the sub-model of the stabilizer system, and (d) the sub-model of the rear axle with dampers.

4.3. Steady Static Circular Test Verification

Based on the standard GB/T6323.6-1994, the steady static circular tests were conducted. The specific test method is as follows: firstly, fix the steering wheel angle and the starting circle radius is 15.0 m; then, accelerate slowly at the longitudinal acceleration below 0.25 m/s² until the lateral acceleration reaches 6.5 m/s^2 . Based on the two truck dynamic models, the steady static circular test were carried out, respectively. The simulation settings are the same as the real test conditions. A comparison of the curves of the body roll angle versus the lateral acceleration is shown in Figure 8. α_1

and α_2 are the absolute values of the sideslip angles of the front axle and the rear axle, respectively. In order to facilitate the test and analysis, researchers usually choose evaluation indicators to describe and evaluate the steady-state response of the vehicle according to their own habits. $\alpha_1 - \alpha_2$ is one of the most important evaluation indicators. If $\alpha_1 - \alpha_2 > 0$, the vehicle has under-steer characteristics; if $\alpha_1 - \alpha_2 = 0$, the vehicle has neutral steering characteristics; If $\alpha_1 - \alpha_2 < 0$, the vehicle has over-steer characteristics [43]. A comparison of the curves of $\alpha_1 - \alpha_2$ versus the lateral acceleration is shown in Figure 9. From Figure 9, it can be seen that the simulation results are close to the test results, which proves that the two truck models can reproduce the handling dynamic responses. Figure 9 also shows that the truck has slight over-steer characteristics.

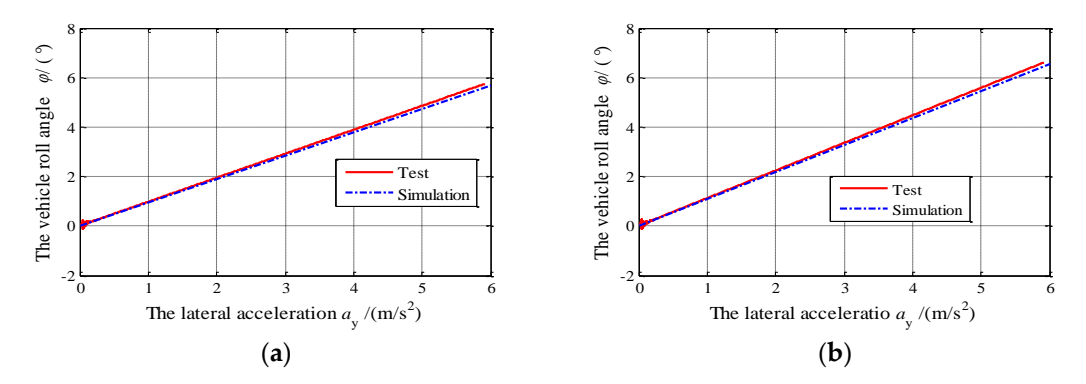


Figure 8. A comparison of the curves of the body roll angle versus the lateral acceleration for the truck with: (a) the multi-leaf spring, and (b) the taper-leaf spring.

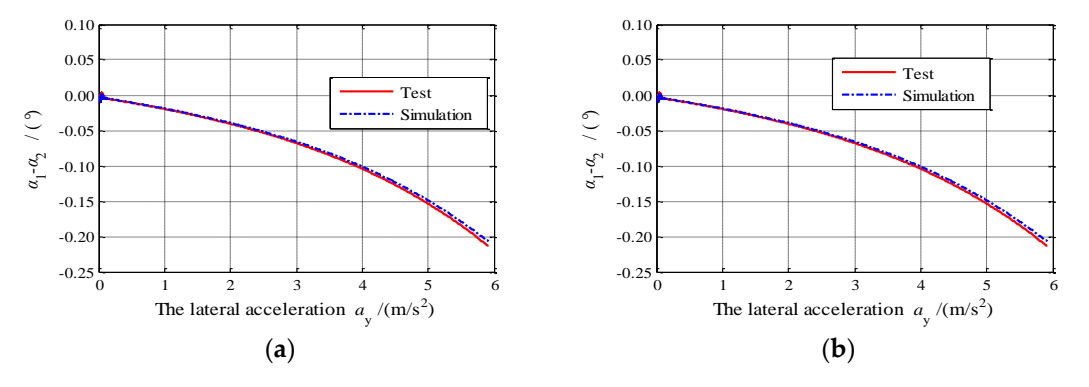


Figure 9. A comparison of the curves of $\alpha_1 - \alpha_2$ versus the lateral acceleration for the truck with: (a) The multi-leaf spring, and (b) the taper-leaf spring.

5. Handling Stability Simulation and Comparison

In general, handling stability tests of vehicles are very dangerous, such as the drift test [43,44]. In order to avoid the potential dangers of handling stability tests, this paper uses simulation methods to carry out the comparative analysis. The changes of the handling stability after replacing the multi-leaf spring with the taper-leaf spring were revealed by the simulations of the drift test, the ramp steer test, and the step steer test.

5.1. Simulation and Comparison of the Drift Tests

The drift test is an important method to study the transient responses of vehicles under the limit operating condition. In the drift simulation, the truck reaches a steady-state condition in the first $10.0 \, \rm s$. A steady-state condition is one in which the truck has the desired steer angle 360° , the initial throttle 20.0, and the initial velocity $40 \, \rm km/h$. In 1.0– $4.0 \, \rm s$, Adams ramps the steering angle from an initial value to the desired value. It then ramps the throttle from $0.0 \, \rm to$ to the full throttle value $100.0 \, \rm from \, 5.0 \, s$ to

10.0 s. Finally, it keeps the throttle fully open from 10.0 s to 15.0 s. The same simulation parameters were set for the two truck models with the multi-leaf spring and the taper-leaf spring, respectively. A comparison of the simulated dynamic responses is shown in Figure 10.0 s.

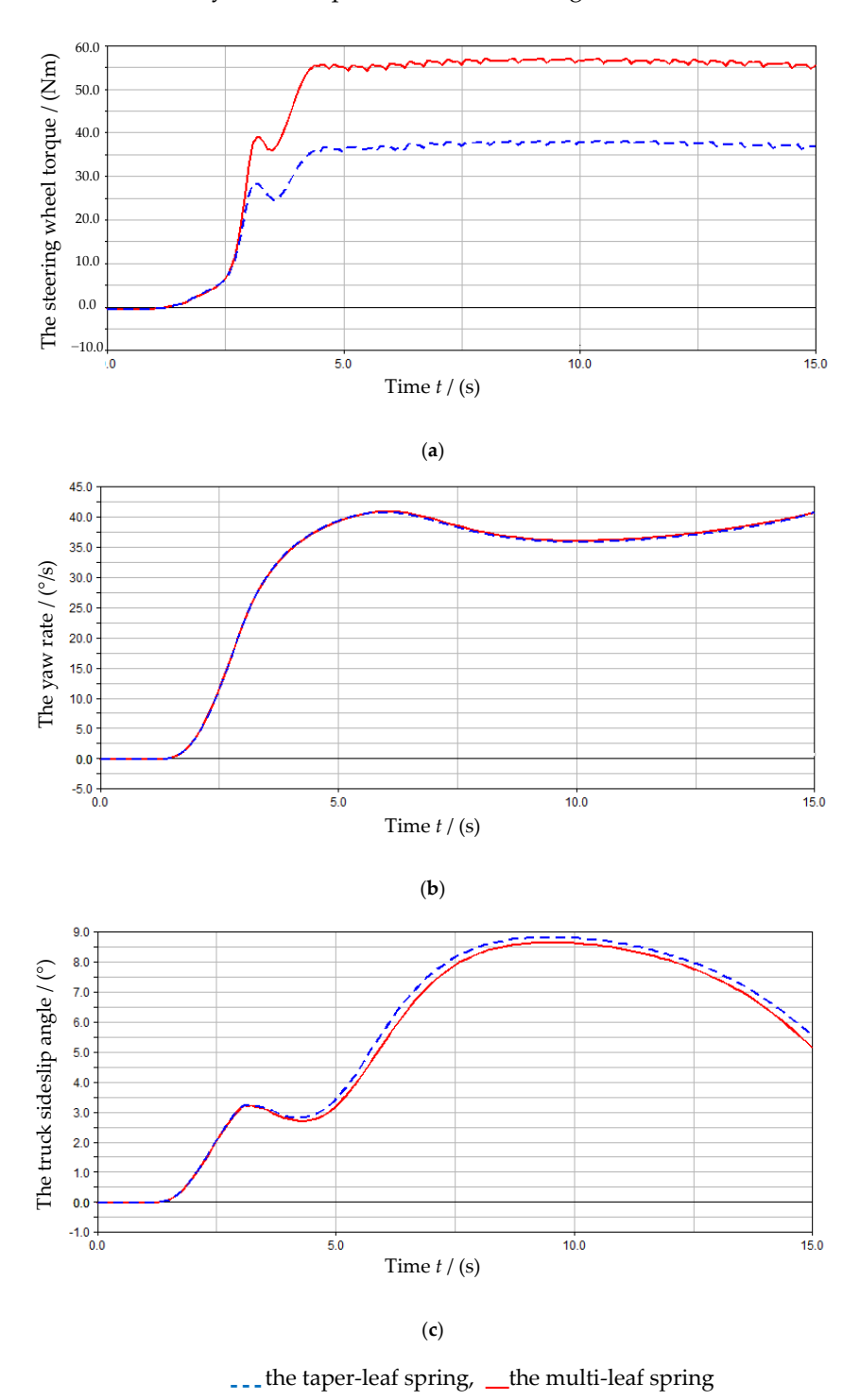


Figure 10. A comparison of the simulated dynamic responses obtained from the drift tests: (a) The steering wheel torque, (b) the yaw rate, and (c) the truck sideslip angle.

From Figure 10a, it can be seen that for the same input, when the steering angle reaches the set value, the steering wheel torque of the truck with the multi-leaf spring suspension is significantly larger than that of the truck with the taper-leaf spring suspension. The result shows that the truck with

the taper-leaf spring suspension has better steering portability than the truck with the multi-leaf spring suspension. From Figure 10b, it can be seen that the two truck models have almost the same yaw rate. The result shows that replacing the multi-leaf spring with the taper-leaf spring has almost no effect on the yaw rate. From Figure 10c, it can be seen that when the steering wheel angle is increased to the set value, the sideslip angles on the basis of the two truck models are almost the same. With the increase of the throttle opening, the sideslip angles on the basis of the two truck models begin to deviate. The sideslip angle of the truck with the taper-leaf spring suspension is obviously larger than that of the truck with the multi-leaf spring suspension. The result shows that the handling of the truck with the taper-leaf spring suspension is poorer than that of the truck with the multi-leaf spring is less 18.8% than that of the multi-leaf spring.

5.2. Simulation and Comparison of the Ramp Steer Tests

In a ramp-steer analysis, time-domain transient response metrics can be obtained [43]. The most important quantities to be measured are: the steering wheel torque, the yaw rate, the truck sideslip angle, and the truck roll angle. During a ramp-steer analysis, Adams ramps up the steering input from an initial value at a specified rate, as shown in Figure 11. The simulations of the ramp steer tests were conducted in Adams based on the two truck models, respectively. The simulation settings are as follows: the initial steer value = 0° , the initial velocity 40 km/h, the ramp = $\tan(\theta) = 15.0$, the start time = 3.0 s, and the end time = 15.0 s. A comparison of the simulated dynamic responses is shown in Figure 12.

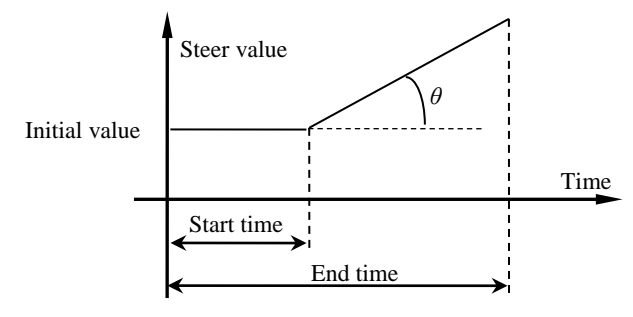


Figure 11. The curve of the input versus the time for the ramp steer test.

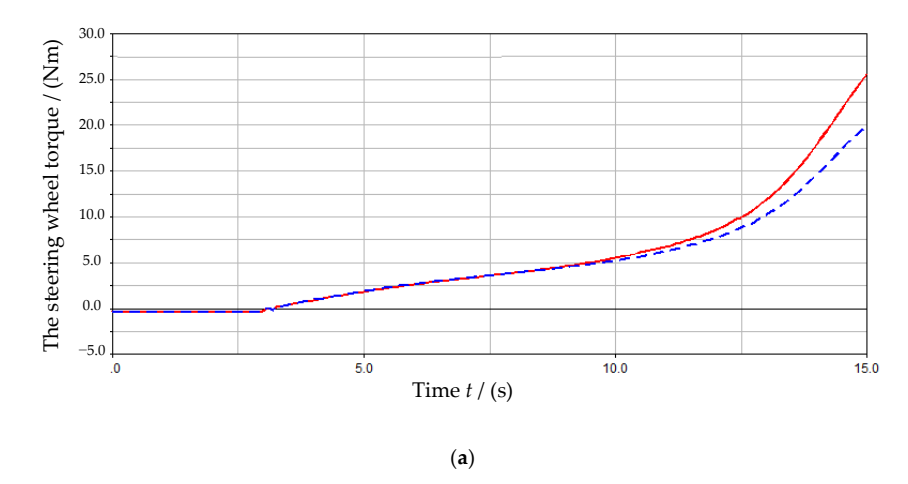


Figure 12. Cont.

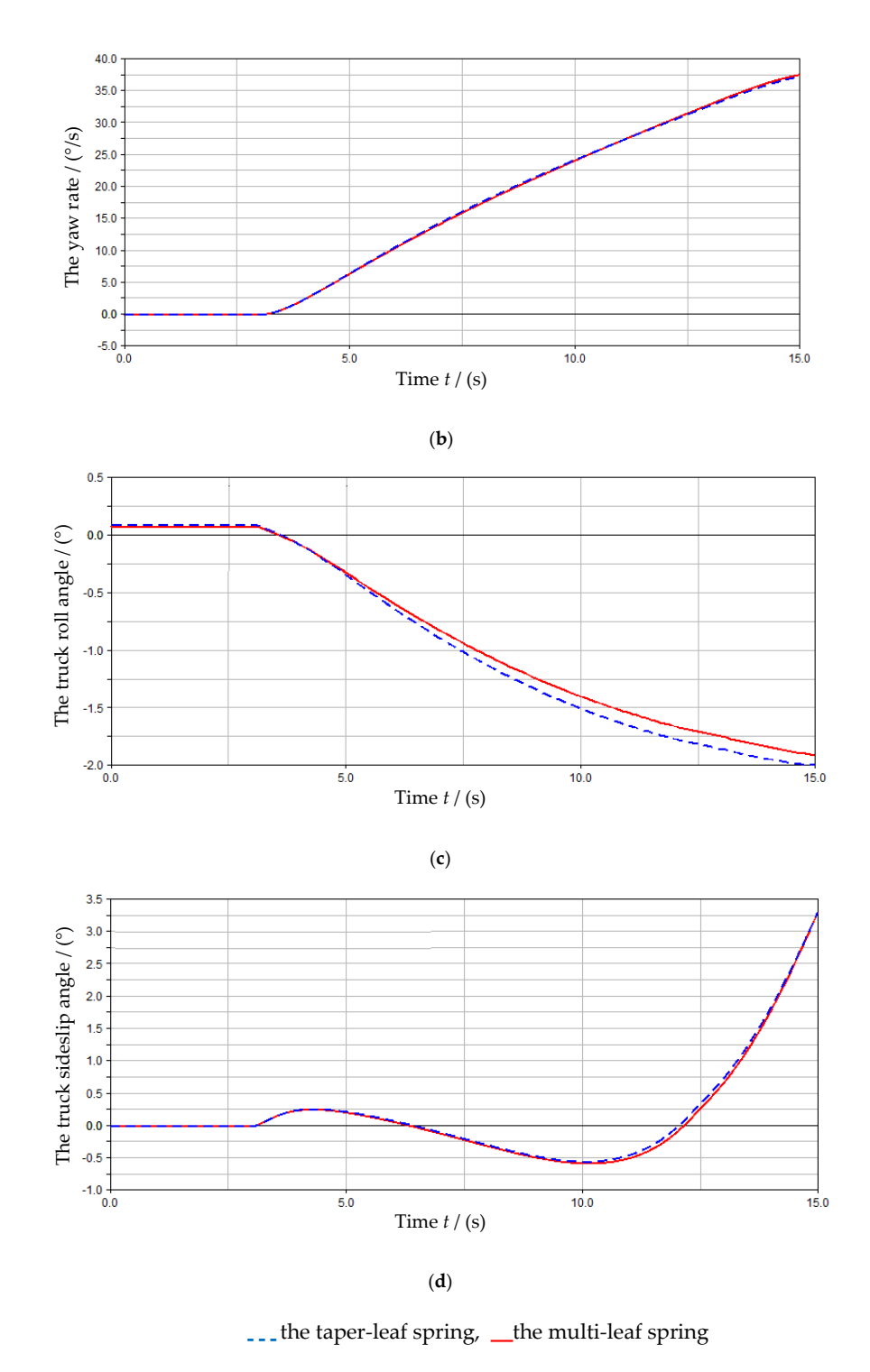


Figure 12. A comparison of the simulated dynamic responses obtained from the ramp steer tests: (a) The steering wheel torque, (b) the yaw rate, (c) the truck roll angle, and (d) the truck sideslip angle.

From Figure 12a, it can be seen that the steering wheel torques from the two truck models are almost the same from the beginning to about 10.0 s. Moreover, in the later stage, with the increasing of the steer angle, the steering wheel torque of the multi-leaf spring truck model increases more obviously. In other words, when the steer angle is very small, the two truck models show almost the same steering portability. However, when the steering angle is very large, the truck with the taper-leaf spring suspension has better steering portability. From Figure 12b, it can be seen that the two truck models show almost the same yaw rate. The result shows that replacing the multi-leaf spring with

the taper-leaf spring has almost no effect on the yaw rate. From Figure 12c, it can be seen that the truck roll angles on the basis of the two truck models are almost the same from 0.0 s to 5.0 s. With the increase of the steer value, the truck roll angles on the basis of the two truck models begin to deviate. The truck roll angle of the truck with the taper-leaf spring suspension is obviously larger than that of the truck with the multi-leaf spring suspension. The results show that the truck with the multi-leaf spring suspension has the stronger stability. From Figure 12d, it can be seen that the two truck models show almost the same sideslip angle. The result shows that replacing the multi-leaf spring with the taper-leaf spring has almost no effect on the truck sideslip angle during the ramp steer test.

5.3. Simulation and Comparison of the Step Steer Tests

The purpose of the step steer test is to characterize the transient response behaviors of vehicles [44]. The steering input ramps up from an initial steer value to the maximum steer value, as shown in Figure 13. During the step steer test, the steady state of the truck changes from the straight driving to the circular motion and the transition between the two steady-state movements is the transient response. The simulations of the step steer tests were conducted in Adams based on the two truck models, respectively. According to Chinese GB/T6323.2-94, the simulation settings are as follows: the initial steer value = 0° , the step start time 2.0 s, the duration time 6.0 s, the end time 30.0 s, and the final steer value 100.0° . A comparison of the simulated dynamic responses is shown in Figure 14.

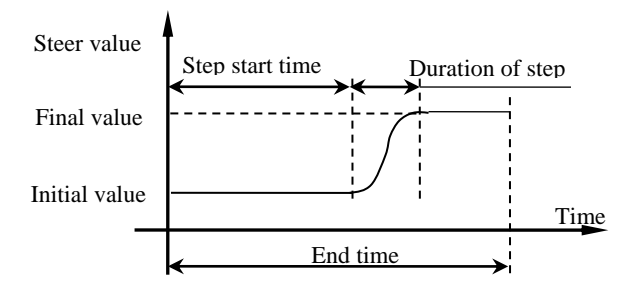


Figure 13. The curve of the input versus the time for the step steer test.

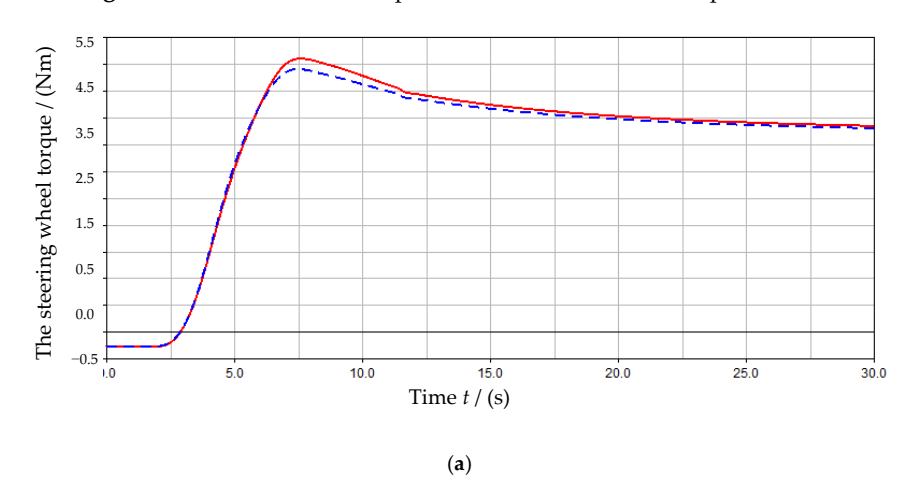


Figure 14. Cont.

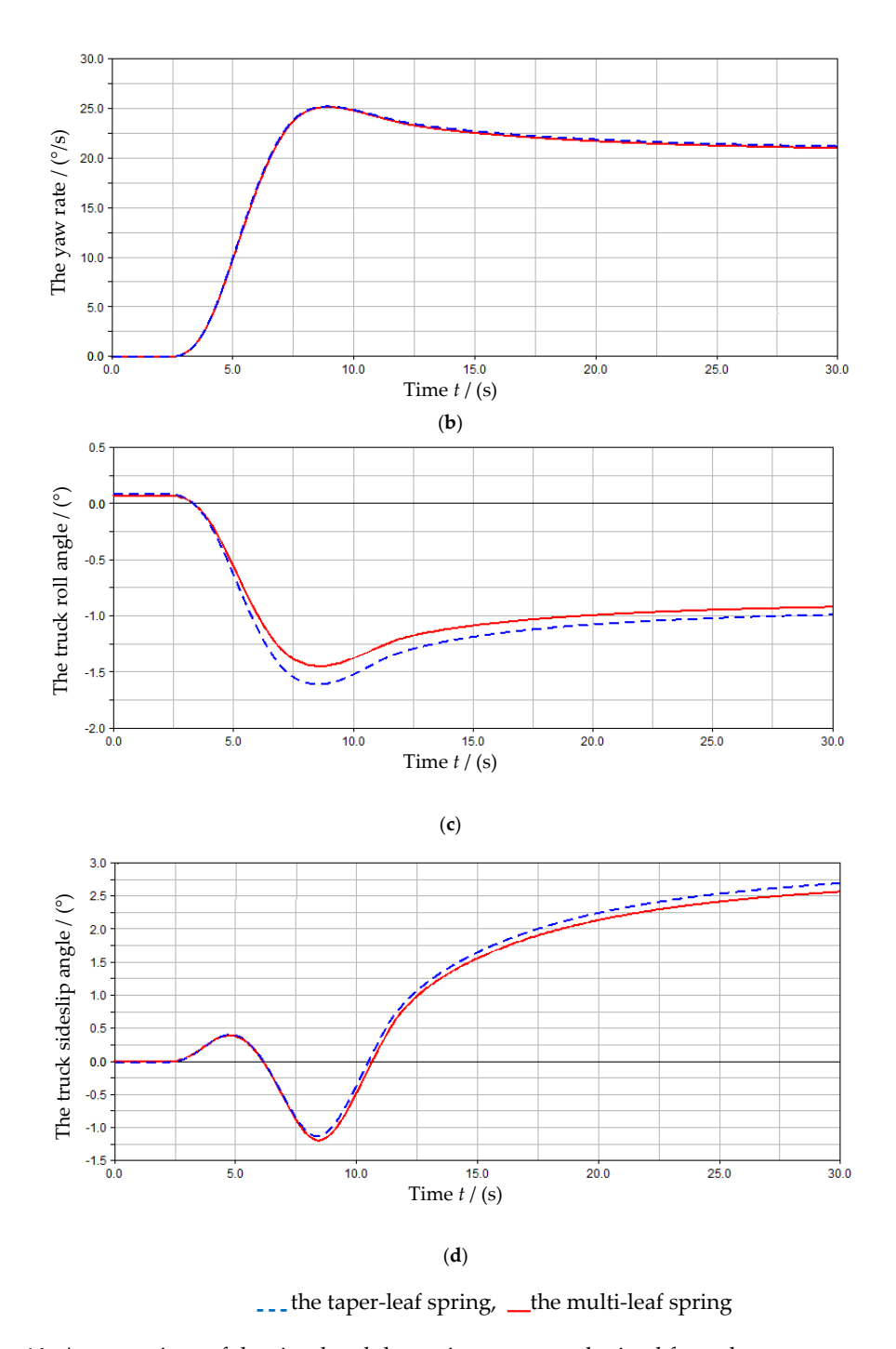


Figure 14. A comparison of the simulated dynamic responses obtained from the step steer tests: (a) The steering wheel torque, (b) the yaw rate, (c) the truck roll angle, and (d) the truck sideslip angle.

From Figure 14a, it can be seen that the steering wheel torques from the two truck models are basically the same from 0.0 s to about 6.5 s. The steering wheel torque of the truck with the taper-leaf spring suspension is slightly smaller than that of the truck with the multi-leaf spring suspension from 20.0 s to 30.0 s. Moreover, the steering wheel torque of the truck with the taper-leaf spring suspension is obviously smaller than that of the truck with the multi-leaf spring suspension from 6.5 s to 20.0 s. The results prove that the truck with the taper-leaf spring suspension has better steering portability during the step steer test. From Figure 14b, it can be seen that the two truck models show almost the same yaw rate during the step steer test. The result further shows that replacing the multi-leaf spring with the taper-leaf spring has almost no effect on the yaw rate. From Figure 14c, it can be seen that the

truck roll angles on the basis of the two truck models are almost the same from 0.0 s to 3.0 s during the step steer test. With the increase of the steer value, the roll angle of the truck with the taper-leaf spring increases more obviously. The results show that the truck with the taper-leaf spring suspension has the poorer stability. Figure 14d illustrates that the sideslip angle of the truck with the taper-leaf spring suspension is obviously larger than that of the truck with the multi-leaf spring suspension. The result further shows that the truck handing performs worse after replacing the multi-leaf spring with the taper-leaf spring.

5.4. Simulation and Comparison of the Braking-in-Turn Tests

The braking-in-turn analysis is one of the most critical analyses encountered in everyday driving. This analysis examines path and directional deviations caused by sudden braking during cornering. Typical results collected from the braking-in-turn analysis include the steering wheel torque, the yaw rate, and the truck sideslip angle [40]. The simulations of the braking-in-turn tests were conducted in Adams based on the two truck models, respectively. According to the international standard ISO7975-85, the simulation settings are as follows: the brake deceleration 6.3 m/s², the lateral acceleration 5.1 m/s², the turn radius 30.0 m, the maximum brake duration 5.0 s, the initial straight-line distance 15.0 m. Figure 15 provides the simulation diagram of the braking-in-turn test based on Adams. Figure 16 provides a comparison of the simulated dynamic responses. From Figure 16a, it can be seen that the steering wheel torques from the two truck models are basically the same. Figure 16b depicts that there are almost no differences for the yaw rate. Figure 16c shows that the sideslip angle of the truck with the taper-leaf spring suspension is almost the same as that of the truck with the multi-leaf spring suspension. From Figure 16d, it can be seen that the two truck models show almost the same bushing longitudinal force at the spring eye during the braking-in-turn test. This proves that the replacement of the leaf spring has little impact on the in-train longitudinal forces during braking.

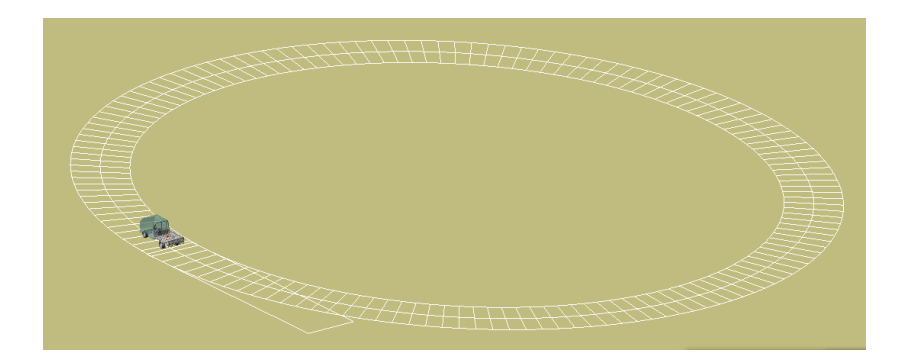
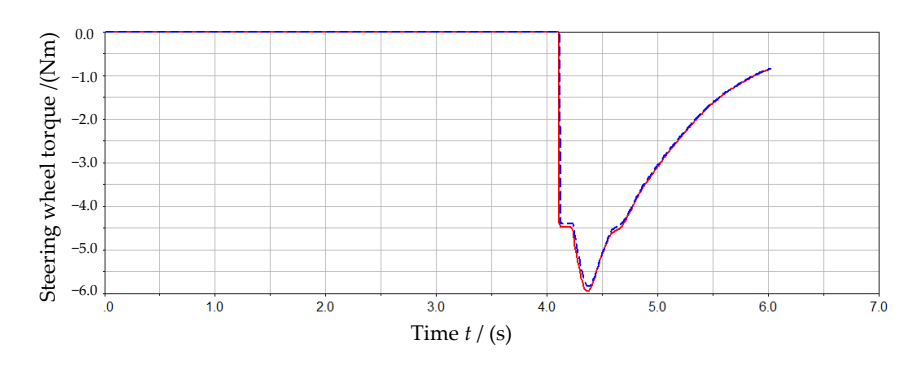


Figure 15. The simulation diagram of the braking-in-turn test based on Adams.



(a) Figure 16. Cont.

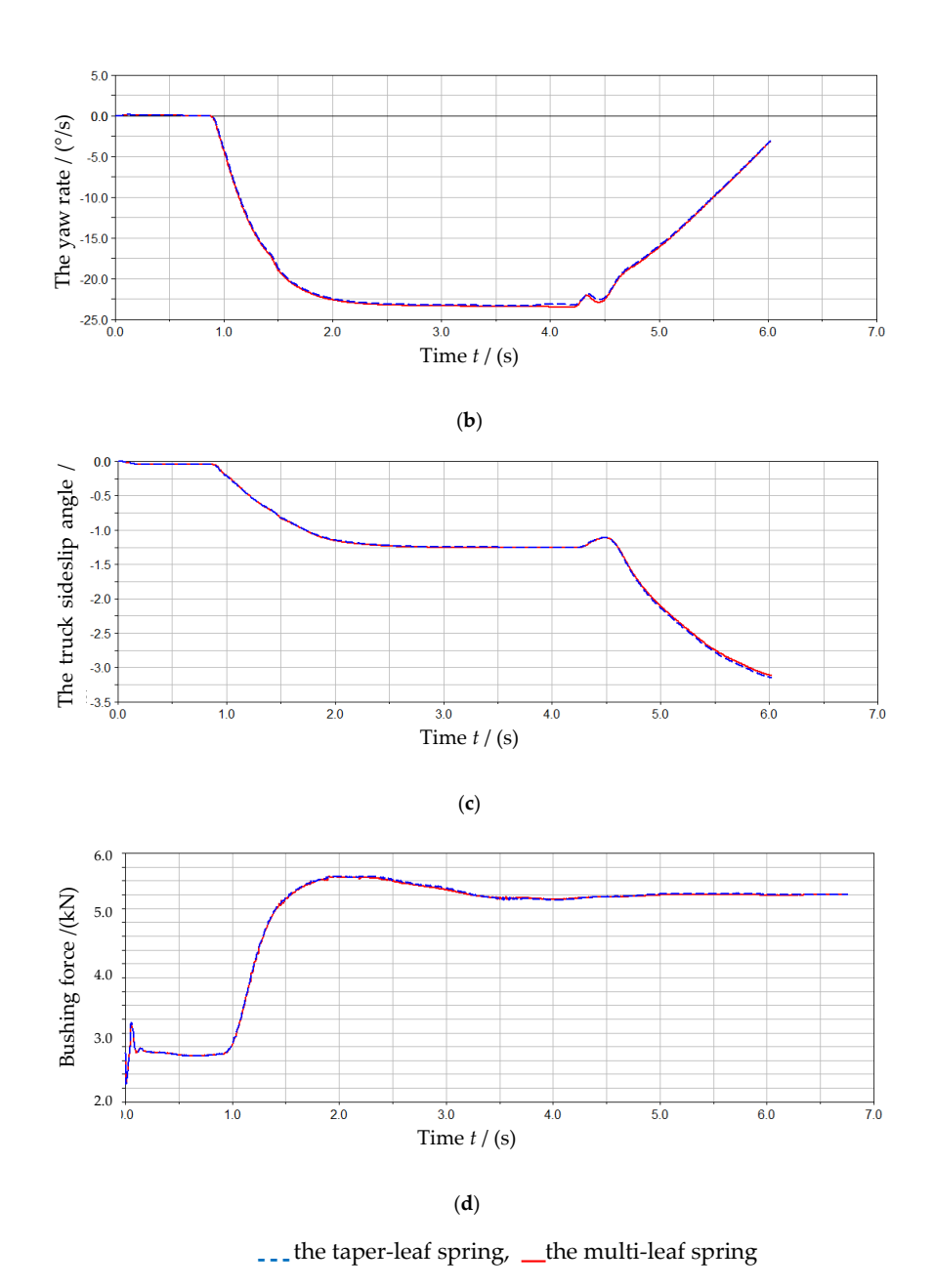
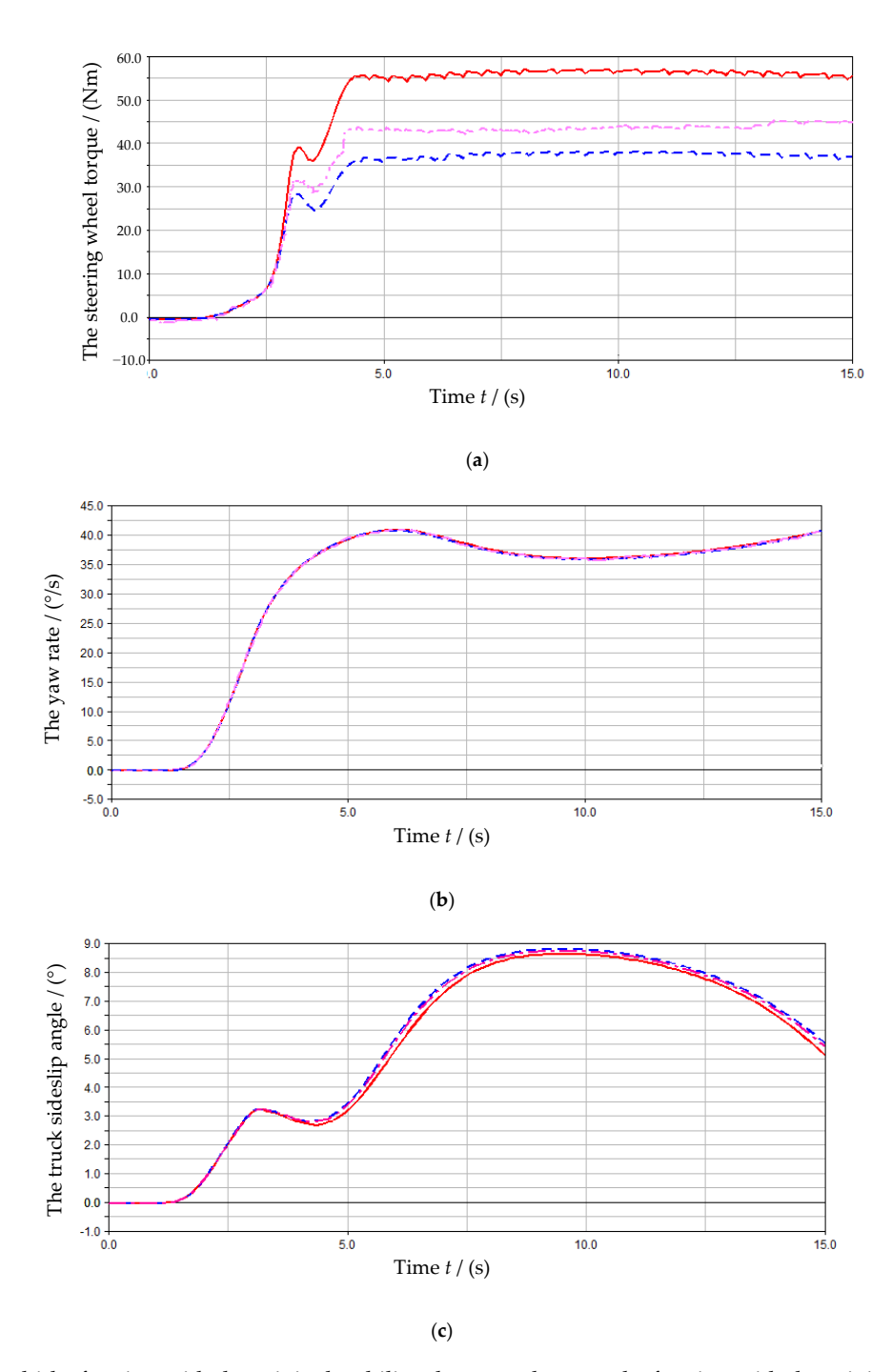


Figure 16. A comparison of the simulated dynamic responses obtained from the step steer tests: (a) The steering wheel torque, (b) the yaw rate, (c) the truck sideslip angle, and (d) the bushing longitudinal force at the spring eye.

6. Analysis on the Reason of Suspension Performance Differences for the Two Leaf Springs

In Section 5, the differences of the simulated dynamic responses for the handling stability should be related to that the torsional stiffness of the two leaf springs. To prove it, the influence of the stabilizer bar on suspension performance with the two leaf springs should be revealed. Thus, the drift simulation test was conducted. The stabilizer bar stiffness is increased by 1.2 times. The other simulation settings are the same as those in Section 5.1. A comparison of the simulated dynamic responses is shown in Figure 17. From Figure 17a, it can be seen that after increasing the stiffness of stabilizer bar, the steering wheel torque for the taper-leaf spring is closer to that for the multi-leaf spring with the original stabilizer bar. Figure 17b shows that the yaw rate for the taper-leaf spring is almost unchanged after increasing the stiffness of stabilizer bar. Figure 17c illustrates that the truck sideslip angle for the taper-leaf spring becomes smaller after increasing the stiffness of stabilizer bar. Moreover, after increasing the stiffness of stabilizer bar, the truck sideslip angle for the taper-leaf spring is more

consistent with that for the multi-leaf spring with the original stabilizer bar. The comparison results show that the torsional stiffness of the two leaf springs have a certain impact on the handling stability.



__the multi-leaf spring with the original stabilizer bar, ___the taper-leaf spring with the original stabilizer bar, ___the taper-leaf spring with increasing the stabilizer bar stiffness

Figure 17. A comparison of the simulated dynamic responses obtained from the drift tests: (a) The steering wheel torque, (b) the yaw rate, and (c) the truck sideslip angle.

7. Conclusions

To reveal the changes of the handling stability after the replacement, the simulations and comparison of the taper-leaf and the multi-leaf spring suspensions with the same vertical stiffness for trucks were conducted. The main innovations and achievements of this paper are as follows:

- (1) An analytical method of replacing the multi-leaf spring with the taper-leaf spring for trucks was proposed.
 - (2) The dynamic models of the truck before and after the spring replacement were established.
- (3) The changes of the handling stability after replacing the multi-leaf spring with the taper-leaf spring were revealed by the simulations of the drift test, the ramp steer test, and the step steer test.

Both the proposed method and the established model were validated by test. The simulation results show that the yaw rate of the truck almost does not change, the steering wheel moment decreases, the vehicle roll angle obviously increases, and the vehicle side slip angle slightly increases after the replacement. The main reason should be related to that the torsional stiffness of the taper-leaf spring is less than that of the multi-leaf spring.

This paper provides a useful reference for the design, modeling, and simulation of the taper-leaf spring suspension system for trucks.

Author Contributions: The corresponding author C.Z. proposed this research, Y.Z. designed the spring experiments; X.L. and Y.Y. performed the truck experiments; H.L. and L.Z analyzed the test data and conducted the simulations; C.Z. reviewed and edited the manuscript; and L.Z. wrote the paper. All authors have read and agreed to the published version of the manuscript.

Funding: This work was supported by the National Natural Science Foundation of China (51575325), Scientific Research Starting Foundation for Doctors (419067), and the School-Enterprise Cooperation Project (2018-KJ-4).

Conflicts of Interest: The authors declare no conflict of interest.

References

- 1. Sun, Y.; Guo, K.; Xu, Z. Research on electronic stability control system testing and evaluation methods for commercial vehicles. *Autom. Technol.* **2018**, *4*, 52–57.
- 2. Jaafari, S.M.M.; Shirazi, K.H. Integrated vehicle dynamics control via torque vectoring differential and electronic stability control to improve vehicle handling and stability performance. *J. Dyn. Syst. Meas. Control* **2018**, *140*, 13. [CrossRef]
- 3. Wan, Y.; Zhao, W.; Feng, R.; Ling, J.; Zong, C.; Zheng, H. Dynamic modeling and vehicle-liquid coupling characteristic analysis for tank trucks. *J. Jilin Univ.* **2017**, *47*, 353–364.
- 4. Zhao, L.; Yu, Y.; Zhou, C.; Wang, S.; Yang, F.; Wang, S. A hydraulic semi-active suspension based on road statistical properties and its road identification. *Appl. Sci.* **2018**, *8*, 740. [CrossRef]
- 5. Li, S.; Yang, S.; Chen, L. Investigation on cornering brake stability of a heavy-duty vehicle based on a nonlinear three-directional coupled model. *Appl. Math. Model.* **2016**, *40*, 6310–6323.
- 6. Santos, J.; Gouveia, R.M.; Silva, F.J.G. Designing a new sustainable approach to the change for lightweight materials in structural components used in truck industry. *J. Clean. Prod.* **2017**, *164*, 115–123. [CrossRef]
- 7. Liu, Y.; Sun, L. Lightweight design on auxiliary frame of mixer truck. *Int. J. U E Serv. Sci. Technol.* **2016**, 9, 207–216. [CrossRef]
- 8. Ashwini, K.; Rao, C.V.M. Design and analysis of leaf spring using various composites-An overview. *Mater. Today Proc.* **2018**, *5*, 5716–5721. [CrossRef]
- 9. Wang, F.; Zhou, C.C.; Yu, Y.W. Analytical calculation method of stiffness and stress for few-chip root-intensive parabolic leaf spring. *J. Shandong Univ. Technol.* **2019**, *33*, 45–50.
- 10. Sert, E.; Boyraz, P. Optimization of suspension system and sensitivity analysis for improvement of stability in a midsize heavy vehicle. *Eng. Sci. Technol. Int. J.* **2017**, *20*, 997–1012. [CrossRef]
- 11. Gu, Y.; Dong, F. Handling stability simulation and test research on an 8×4 type construction truck. *Int. J. Control Autom.* **2016**, *9*, 403–410.
- 12. Huan, X.; Zhang, X. Numerical study of disturbance force effect on handing stability for electric-driven articulated truck in a straight-line. *Source UPB Sci. Bull. Ser. D Mech. Eng.* **2018**, *80*, 55–68.

Appl. Sci. 2020, 10, 1293 20 of 21

13. Anchukov, V.; Alyukov, A.; Aliukov, S. Stability and control of movement of the truck with automatic differential locking system. *Eng. Lett.* **2019**, 27, 131–139.

- 14. Duan, L.; Song, C.; Yang, S.; Fan, S.; Lu, B. High-precision modeling and simulation of the taper leaf spring of tandem suspension of commercial vehicles. *J. Mech. Sci. Technol.* **2016**, *30*, 3061–3067. [CrossRef]
- 15. Moon, I.D.; Yoon, H.S.; Oh, C.Y. A flexible multi-body dynamic model for analyzing the hysteretic characteristics and the dynamic stress of a taper leaf spring. *J. Mech. Sci. Technol.* **2006**, 20, 1638–1645. [CrossRef]
- 16. Wang, C.; Shi, W.; Zu, Q. Calculation and analysis of stiffness of taper-leaf spring with variable stiffness. *SAE Tech. Pap.* **2014**. [CrossRef]
- 17. Zhou, S.; Huang, H.; Ouyang, L. Analysis and computation of taper leaf spring based on FE contact analysis. *Adv. Mater. Res.* **2013**, 705, 516–522. [CrossRef]
- 18. Kim, B.M.; Kim, J.W.; Moon, I.D.; Oh, C.Y. Optimal combination of design parameters for improving the kinematics characteristics of a midsize truck through design of experiment. *J. Mech. Sci. Technol.* **2014**, *28*, 963–969. [CrossRef]
- 19. Chandra, H.; Pratiwi, D.K.; Zahir, M. High-temperature quality of accelerated spheroidization on SUP9 leaf spring to enhance machinability. *Heliyon* **2018**, *4*, e01076. [CrossRef]
- 20. Fragoudakis, R.; Savaidis, G.; Nikolaos, M. Optimizing the development and manufacturing of 56SiCr7 leaf springs. *Int. J. Fatigue* **2017**, *103*, 168–175. [CrossRef]
- 21. Kumar, K.; Aggarwal, M.L. Optimization of various design parameters for EN45A flat leaf spring. *Mater. Today Proc.* **2017**, *4*, 1829–1836. [CrossRef]
- 22. Jenarthanan, M.P.; Ramesh Kumar, S.; Venkatesh, G.; Nishanthan, S. Analysis of leaf spring using Carbon /Glass Epoxy and EN45 using ANSYS: A comparison. *Mater. Today Proc.* **2018**, *5*, 14512–14519. [CrossRef]
- 23. Ozmen, B.; Altiok, B.; Guzel, A.; Kocyigit, I.; Atamer, S. A novel methodology with testing and simulation for the durability of leaf springs based on measured load collectives. *Procedia Eng.* **2015**, *101*, 363–371. [CrossRef]
- 24. Duruş, M.; Kırkayak, L.; Ceyhan, A.; Kozan, K. Fatigue life prediction of Z type leaf spring and new approach to verification method. *Procedia Eng.* **2015**, *101*, 143–150. [CrossRef]
- 25. Bakir, M.; Ozmen, B.; Donertas, C. Correlation of simulation, test bench and rough road testing in terms of strength and fatigue life of a leaf spring. *Procedia Eng.* **2018**, *213*, 303–312. [CrossRef]
- 26. Kong, Y.S.; Abdullah, S.; Omar, M.Z.; Haris, S.M. Failure assessment of a leaf spring eye design under various load cases. *Eng. Fail. Anal.* **2016**, *63*, 146–159. [CrossRef]
- 27. Bi, S.; Li, Y.; Zhao, H. Fatigue analysis and experiment of leaf-spring pivots for high precision flexural static balancing instruments. *Precis. Eng.* **2019**, *55*, 408–416. [CrossRef]
- 28. Malikoutsakis, M.; Savaidis, G.; Savaidis, A.; Ertelt, C.; Schwaiger, F. Design, analysis and multi-disciplinary optimization of high-performance front leaf springs. *Theor. Appl. Fract. Mech.* **2016**, *83*, 42–50. [CrossRef]
- 29. Liu, Z.; Li, Y.; Hong, L. The effect of hinger on performance of front taper-leaf spring suspension of commercial truck. *J. Jilin Univ.* **2014**, 44, 11–16.
- 30. Liu, N.; Zhao, D.; Gu, J.; Mu, P. Research on main leaf center trajectory of taper leaf spring and suspension kinematics analysis. *Automob. Technol.* **2019**, *11*, 42–46.
- 31. Termous, H.; Shraim, H.; Talj, R. Coordinated control strategies for active steering, differential braking and active suspension for vehicle stability, handling and safety improvement. *Veh. Syst. Dyn.* **2019**, *57*, 1494–1529. [CrossRef]
- 32. Li, H.; Li, S.; Sun, W. Vibration and handling stability analysis of articulated vehicle with hydraulically interconnected suspension. *J. Vib. Control* **2019**, 25, 1899–1913. [CrossRef]
- 33. Zhang, L.; Zhang, S.; Zhang, W. Multi-objective optimization design of in-wheel motors drive electric vehicle suspensions for improving handling stability. *Proc. Inst. Mech. Eng. Part D J. Automob. Eng.* **2019**, 233, 2232–2245. [CrossRef]
- 34. Bagheri, M.R.; Mosayebi, M.; Mahdian, A.; Keshavarzi, A. Multi-objective optimization of double wishbone suspension of a kinestatic vehicle model for handling and stability improvement. *Struct. Eng. Mech.* **2018**, *68*, *633*–*638*.
- 35. Li, G.; Liu, F.; Tan, R.; Li, X.; Wang, T. Mathematical model of vehicle handling stability based on suspension K&C characteristics parameters. *China Mech. Eng.* **2018**, 29, 1316–1323.
- 36. Ahmadian, M. Magneto-rheological suspensions for improving ground vehicle's ride comfort, stability, and handling. *Veh. Syst. Dyn.* **2017**, *55*, 1618–1642. [CrossRef]

Appl. Sci. 2020, 10, 1293 21 of 21

37. Zhou, C.C.; Zhao, L.L. *Analytical Calculation Theory of Vehicle Suspension Elasticity*; Machinery Industry Press: Beijing, China, 2012.

- 38. Meng, Y.; Gan, X.; Wang, Y.; Gu, Q. LQR-GA controller for articulated dump truck path tracking system. *J. Shanghai Jiaotong Univ.* **2019**, 24, 78–85. [CrossRef]
- 39. Gu, Z.; Mi, C.; Ding, Z.; Zhang, Y.; Liu, S.; Nie, D. An energy-based fatigue life prediction of a mining truck welded frame. *J. Mech. Sci. Technol.* **2016**, *30*, 3615–3624. [CrossRef]
- 40. Chen, J. *MSC. Adams-Examples of Technical and Engineering Analysis*; China Water Resources and Hydropower Press: Beijing, China, 2008.
- 41. Lu, Y.; Zheng, W.; Chen, E.; Zhang, J. Research on ride comfort and safety of vehicle under limited conditions based on dynamical tire model. *J. Vibroengineering* **2017**, *19*, 1241–1259. [CrossRef]
- 42. Bibin, S.; Pandey, A.K. A hybrid approach to model the temperature effect in tire forces and moments. *SAE Int. J. Passeng. Cars Mech. Syst.* **2017**, *10*, 25–37. [CrossRef]
- 43. Gupta, A.; Ghosh, B.; Balasubramanian, A.; Patil, S.; Raval, C. Reducing brake steer which causes vehicle drift during braking. *SAE Tech. Pap.* **2019**. No. 2019-26-0072. [CrossRef]
- 44. Yamauchi, S.; Kioka, W.; Kitano, T. Drifting motion of vehicles in tsunami inundation flow. *Procedia Eng.* **2015**, *116*, 592–599. [CrossRef]



© 2020 by the authors. Licensee MDPI, Basel, Switzerland. This article is an open access article distributed under the terms and conditions of the Creative Commons Attribution (CC BY) license (http://creativecommons.org/licenses/by/4.0/).